Magnetic topologies of an in vivo FTE observed by Double Star/TC-1 at Earth's magnetopause

Z. Y. Pu,[1] J. Raeder,[2] J. Zhong,[1] Y. V. Bogdanova,[3,4] M. Dunlop,[4] C. J. Xiao,[5] X. G. Wang,[5] and A. Fazakerley[3]

Received 3 June 2013; revised 30 June 2013; accepted 1 July 2013; published 26 July 2013.

[1] Flux transfer events (FTEs) are magnetic flux ropes formed at planetary magnetopauses (MPs). Although evidence suggests that FTEs form through time-dependent magnetic reconnection, details of that process and 3D structure of the flux ropes remain largely unclear. This letter presents Double Star/TC-1 data of an FTE occurred on 7 April 2004 which show that the FTE was separated by two X-lines moving south-dawnward. In particular, the electron energy-pitch angle distribution implies that the FTE was composed of flux ropes of all four possible magnetic topologies, indicating that the field lines must have reconnected multiple times. This is an intrinsic property of FTEs formed by 3D multiple X-line reconnection distinguished from quasi 2D FTE models. This knowledge of FTE magnetic topologies helps to improve our understanding of solar wind- magnetosphere coupling at the MP. **Citation:** Pu, Z. Y., J. Raeder, J. Zhong, Y. V. Bogdanova, M. Dunlop, C. J. Xiao, X. G. Wang, and A. Fazakerley (2013), Magnetic topologies of an in vivo FTE observed by Double Star/TC-1 at Earth's magnetopause, *Geophys. Res. Lett.*, *40*, 3502–3506, doi:10.1002/grl.50714.

1. Introduction

[2] Flux transfer events (FTEs) [*Russell and Elphic*, 1978] are magnetic flux ropes formed at the magnetopause (MP), allowing solar wind energy and plasma to be transported into the magnetosphere [*Paschmann et al*., 1982]. Despite of many years of research [e.g., *Russell and Elphic*, 1978; *Lee and Fu*, 1985; *Scholer*, 1988; *Liu and Hu*, 1988; *Scholer*, 1995 and references therein; *Cooling et al*., 2001], the three-dimensional (3D) structure of FTEs and their formation mechanism are still largely unknown. In situ observations [*Hasegawa et al*., 2010; *Trenchi et al*., 2011; *Oieroset et al*., 2011; *Zhang et al*., 2012] have found in vivo (active) FTEs flanked by two converging flows towards the central flux rope in the MP current layer, which is considered to be consistent with the FTE formation via multiple sequential X-line reconnection (MSXR) [*Raeder*, 2006]. Global simulations have shown a few possible generation paradigms with complicated 3D FTE configurations [*Fedder et al*., 2002; *Raeder*, 2006; *Dorelli and Bhattacharjee*, 2009; *Tan et al*., 2011; *Rastätter et al*., 2012]. Of particular interest in the simulations is the finding that a 3D FTE flux rope may illustrate four types of magnetic topologies for connection to the Earth and the magnetosheath (MSH): (i) open flux connecting southern hemisphere to the MSH, (ii) open flux connecting the MSH to northern hemisphere, (iii) close flux connecting both hemispheres, and (iv) the MSH flux [*Tan et al*., 2011; *Rastätter et al*., 2012], which was first revealed in a 3D local MHD simulation of multiple X-line reconnection long time ago [*Fu et al.*, 1990]. Magnetic topologies of FTE flux ropes have significant impact on solar wind-magnetosphere interaction [*Eastwood et al*., 2012]. This paper reports Double Star/TC-1 measurements [*Liu et al*., 2005] of an in vivo FTE occurring on 7 April 2004. The observations present the first in situ evidence of co-existence of four types of magnetic topologies within the FTE flux rope, confirming this intrinsically 3D nature of MP reconnection [*Fu et al*., 1990; *Tan et al*., 2011; *Rastätter et al*., 2012]. The magnetic field, plasma and electron data used are taken from the FGM, HIA, and PEACE instruments [*Carr et al*., 2005; *Reme et al*., 2005; *Fazakerley et al*., 2005] on board TC-1. Geocentric Solar Ecliptic (GSE) coordinates are used throughout this study.

2. Observations

2.1. Overview of the Event

[3] From 22:00 to 23:00 UT on 7 April 2004, TC-1 travelled inbound from the MSH into the magnetosphere, crossing the southern/dawnside MP at ~ (9.6, −6.0, −1.3) R_E (Earth radii). Based on the minimum variance analysis of magnetic field measurements [*Sonnerup and Scheible*, 1998], the local MP boundary normal coordinates [*Russell and Elphic*, 1978] are found to be: **L** = (0.41, 0.52, 0.75), **M** = (−0.35, −0.67, 0.66), and **N** = (0.84, −0.54, −0.09), where **N** is perpendicular to the local MP surface outward positive, **L** points to the direction of magnetic field component with maximum variance during the MP crossing, and M = N × L. During this interval, the IMF was essentially southward with a substantial dawnward component. TC-1 detected an FTE during 22:23:20–22:25:10 UT (yellow colored in Figure 1a) based on the bipolar B_N signatures, increase of magnitude of **B**, and mixture of the MSH and magnetospheric (MSP) populations [*Le et al*., 1993]. Figure 1a presents the overview of the observations. From top to bottom are shown the ion energy spectrum; magnetic field and ion velocity in GSE; magnetic field and ion velocity

[1]School of Earth and Space Sciences, Peking University, Beijing, China.
[2]Space Science Center and Physics Department, University of New Hampshire, Durham, New Hampshire, USA.
[3]Mullard Space Science Laboratory, University College London, Dorking, UK.
[4]Rutherford-Appleton Laboratory, Chilton, Oxfordshire, UK.
[5]School of Physics, Peking University, Beijing, China.

Corresponding author: Z. Y. Pu, School of Earth and Space Sciences, Peking University, 5 Yiheyuan St., Haidian, Beijing 100871, China. (zypu@pku.edu.cn)

0094-8276/13/10.1002/grl.50714

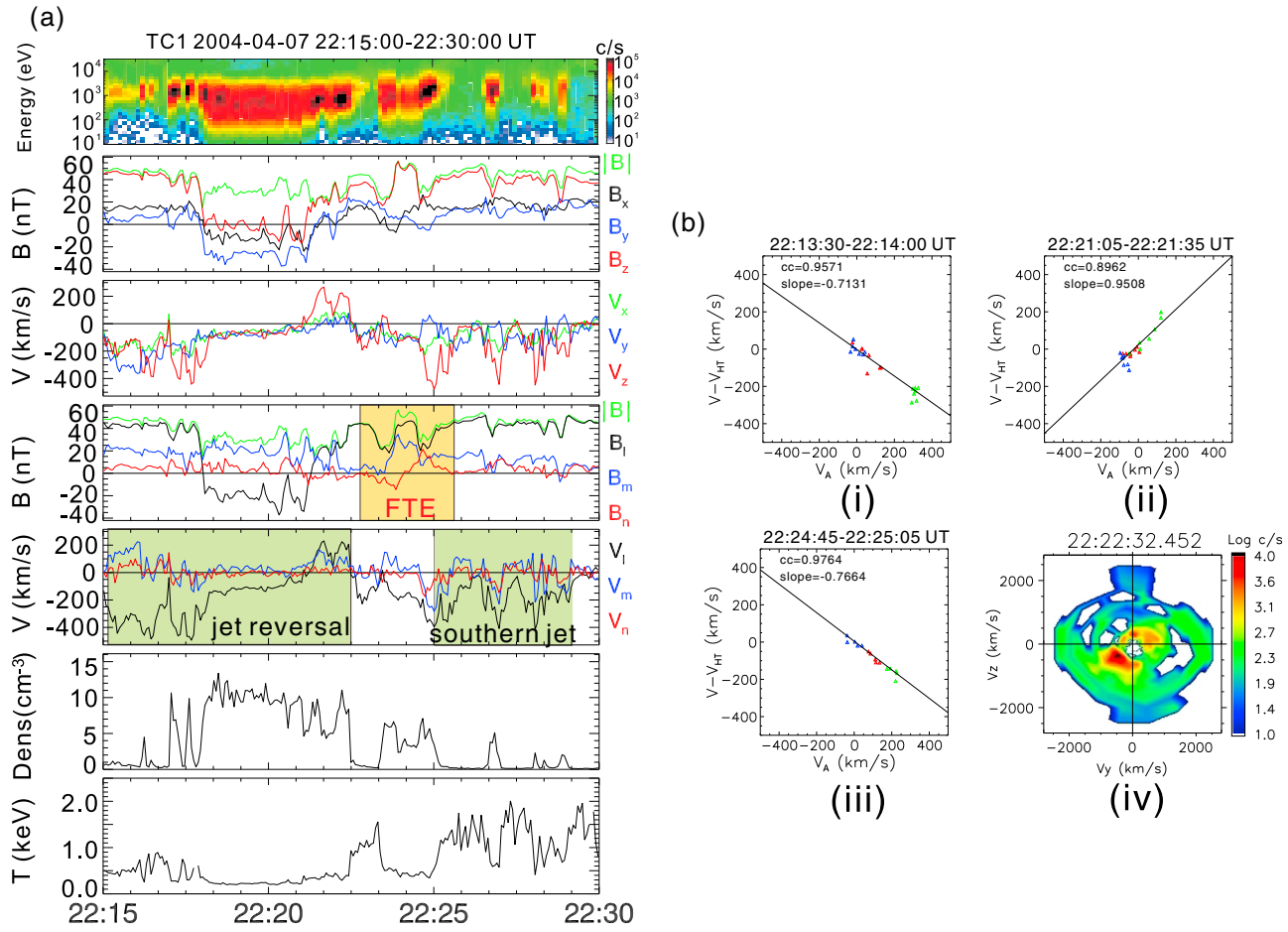

Figure 1. (a). Overview of TC-1 observations of the FTE on 7 April 2004. Figure 1b (i) Walén scatter plot for the time interval when TC-1 recorded the southward jet associated with the X-line ahead the FTE, (ii) similar plot for the period when TC-1 recorded the northward jet of the X-line ahead the FTE, (iii) similar plot for the period when TC-1 recorded the southward jet associated with the X-line behind the FTE. (iv) 3D ion velocity distribution at ~22:22:32, showing the coexistence of weaker south-dawnward flow and stronger northward/duskward flow in the time interval of 22:22:30–22:23:25 UT immediately ahead the FTE.

in (**L,M,N**) coordinates; ion number density and temperature, respectively. Before encountering the FTE, TC-1 detected a pair of southward then northward reversal jet (colored green in Figure 1a) with respect to the background MSH flow of $v_L \sim 150$ km/s south-dawnward. The magnetic field component normal to the local MP (B_N) was essentially positive (negative) when the southward (northward) jet was observed. Figure 2b (i) and (ii) presents the Walén scatter plots [*Sonnerup et al.*, 1987; *Phan et al.*, 2004] of $\mathbf{v} - \mathbf{V_{HT}}$ versus $\mathbf{V_A}$ for the two time intervals when the spacecraft recorded the southward and northward jet, respectively, where $\mathbf{V_A}$ denotes the Alfvén velocity, and $\mathbf{v} - \mathbf{V_{HT}}$ stands for the plasma velocity in the de Hoffmann–Teller (HT) frame [*Khrabrov and Sonnerup*, 1998]. The fact that correlation coefficients close to 1 and slopes of the regression lines are not far from unit indicates a good Alfvénic nature of the boundary flows of the MP reconnection [*Sonnerup et al.*, 1995; *Phan et al.*, 2004]. Based on the classical reconnection picture, TC-1 was passing from the southern to the northern side of the X-line region during the jet reversal [*Moore et al.*, 2002; *Pu et al.*, 2005]. After being swept by the FTE, TC-1 went into the MSP side of boundary layer and persistently observed strong southward flows accompanied by essentially positive B_N. Figure 1b (iii) presents the Walén test plot for a time period during the TC-1 encountering with southward flows. The Walén plot shows again the boundary flow nature of MP reconnection, indicating that the spacecraft came into the outflow region on the southern/dawnside side of the second X-line. Moreover, while TC-1 measured these reconnection flows ahead (behind) the FTE, there was time interval in which the electron energy-pitch angle distribution showed that MSP electrons (with energy $> \sim 1$ keV) were flowing out of the magnetosphere antiparallel (parallel) to the field lines, (not shown here), providing further evidence of open field lines resulting from X-line reconnection at the MP [*Farrugia et al.*, 1987b].

[4] In recent studies, the presence of converging plasma jets toward the center of the flux rope has been regarded as a pronounced signature of in vivo flux ropes flanked by two X-lines [*Hasegawa et al.*, 2010; *Oieroset et al.*, 2011; *Zhang et al.*, 2012]. This is essentially the case that Figures 1a and 1b show. However, immediately prior to the FTE, instead of a north-duskward jet toward the FTE center, TC-1 detected a south-dawnward flow from 22:22:30 to 22:23:25 UT. How can this unexpected phenomenon be explained? It is worthwhile to note that the pair of converging

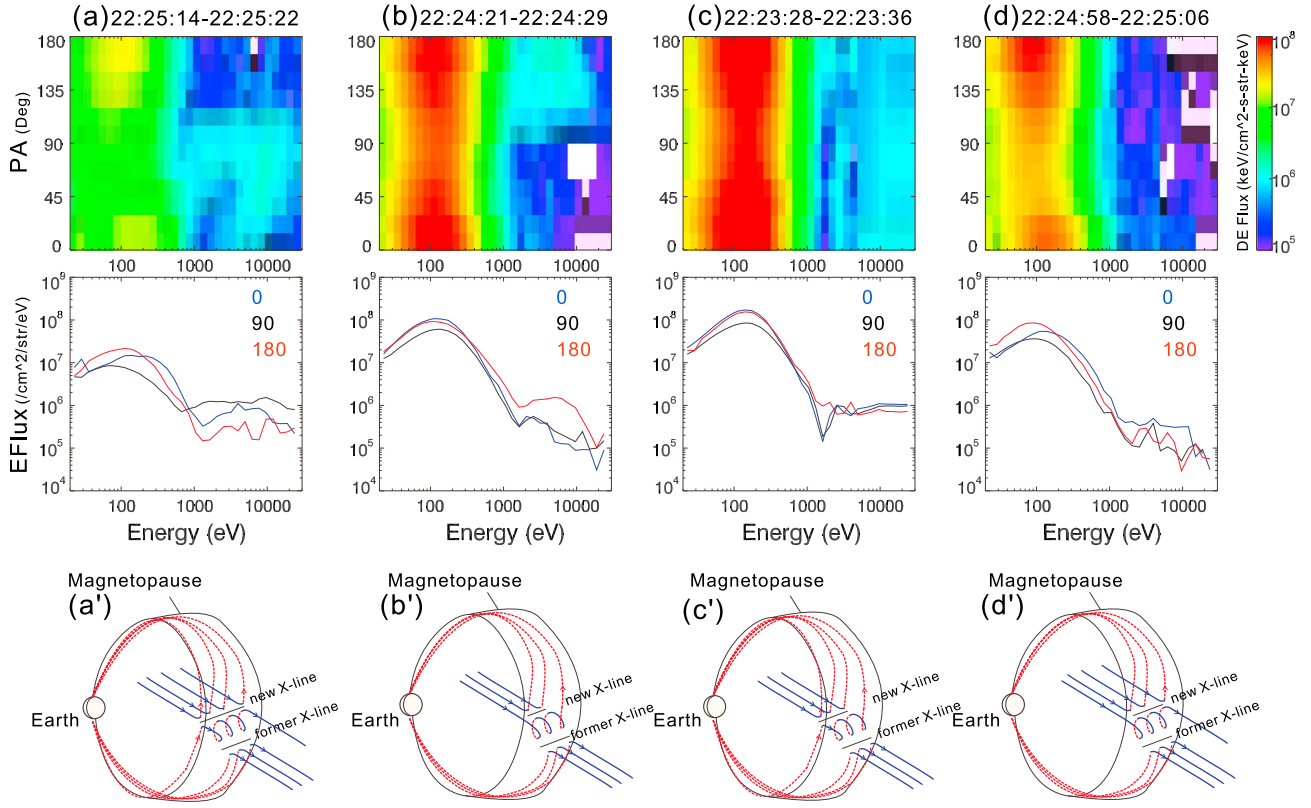

Figure 2. Electron pitch angle distributions of differential energy flux (top row) and energy spectra (second row) measured by the PEACE instrument onboard TC-1 at four times during the FTE 2 crossing. The pitch angle data are 8 s averages, and the energy spectra are for pitch angles of 0°, 90°, and 180°, respectively. The bottom row shows schematic representations of the corresponding magnetic topology inferred from the electron data.

jets can only be distinctly measured when spacecraft is located in the MP boundary layer [*Zhang et al*., 2012]. Within the MSH and magnetosphere, FTEs are often observed without such a clear signature. *Zhang et al*. [2012] reported that among 3701 FTE signatures that they identified with THEMIS data in 2007 and 2008, only 41 (~1%) were distinctly seen in association with the flow reversals. By an inspection of Figure 1a, one sees that during the interval of 22:22:30–22:23:25 UT, TC-1 went from the boundary layer into the magnetosphere, where a pair of counter-streaming flows was observed. As clearly illustrated in the 3D ion velocity distribution in Figure 1b (iv), the end of strong south-dawnward flow in association with the X-line behind the FTE dominated over the weak north-duskward flow from the X-line ahead the FTE. It is thus reasonable to expect that if TC-1 had remained in the boundary layer, it would have measured the north-duskward jet as before.

[5] The fact that the FTE is flanked by two X-lines is consistent with the FTE being formed through the multiple X-line reconnection process [*Lee and Fu*, 1985; *Raeder*, 2006]. The L-component separation between the first and second X-line is roughly estimated to be greater than ~6.4 R_E based on timing and MSH flow speed. The scale size of the FTE in the L-direction (estimated based on bipolar B_N time interval times v_L) is about 2.6 R_E. The flux rope orientation is estimated by minimum variance analysis of the magnetic field data [*Farrugia et al*., 1987a] as (0.13, 0.99, 0.03) in GSE which is close to the Y-axis, so that the jets on the southern and northern sides of the FTE lie essentially normal to this rope axis with the intersection angles being ~94.5° and ~97.0°, respectively.

2.2. Electron Pitch Angle-Energy Distributions and Field Line Topologies

[6] The top panel of Figure 2 shows the electron pitch angle-energy distributions from PEACE instrument during the FTE crossing. The middle panel of Figure 2 shows 1D cuts through the electron distributions at 0°, 90°, and 180° pitch angles. There are four types of distinct distributions coexisting in the central FTE: (i) an essentially field-aligned (0–90° pitch angle) MSP population (>1 keV), accelerated (200–700 eV) field-aligned MSH electrons and antifield-aligned MSH electrons (~100 eV) (first and second panel, a), (ii) an essentially antifield-aligned (90–180° pitch angle) MSP population and counter-streaming (field-aligned/antifield-aligned) MSH electrons (b), (iii) almost isotropic MSP populations combined with slightly energized counter-streaming MSH electrons of high intensity (c), and (iv) heated MSH electrons (>200 eV) and much lower flux of MSP populations (d). The first and second type distributions suggest an open field line geometry connecting the southern magnetosphere (third panel, column a) and northern magnetosphere (b) to the MSH, respectively [*Farrugia et al*., 1987b], allowing the escape of MSP energetic electrons into the MSH and entry of the MSH electrons into the magnetosphere, as well as their subsequent reflection. The third and fourth distribution types indicate newly formed closed field lines connecting both hemispheres [*Bogdanova et al*.,

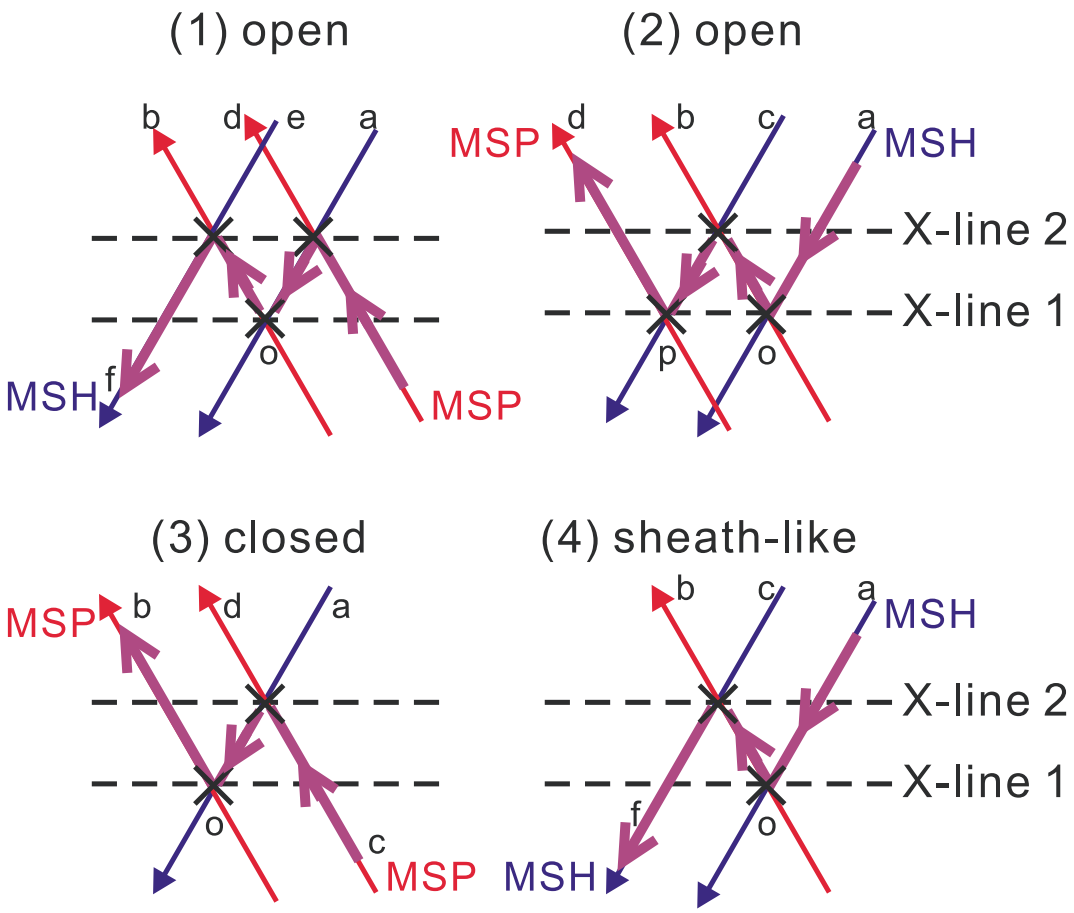

Figure 3. Diagram showing how four types of field line geometries are created in MSXR. X-line 1 represents the first formed equatorial X-line having moved south-dawnward and X-line 2 the newly formed X-line. Magnetic field lines in the magnetosheath (MSH) and magnetosphere (MSP) are in blue and red, respectively. Open field line a-o-b and c-p-d from MSH to the northern MSP are first formed at the X-line 1. FTE and associated four types of field lines (in purple) are produced later when reconnection takes place at X-line 2.

2008] (c), and newly formed MSH field lines (d), respectively. They are created when the reconnected open field lines reconnect, respectively, with the MSP and MSH field lines again; the MSP and MSH electrons are then trapped on newly closed field lines (Figure 2c'), and the accelerated MSH electrons appear on the new MSH field lines (Figure 2d').

3. Discussion and Summary

[7] We have reported an in vivo FTE flanked by two X-lines observed by TC-1 at southern/dawnside MP. The observations are consistent with the scenario of FTE formation through MSXR process [*Raeder*, 2006]. As the IMF with a southward B_z component and a strong B_y component drapes over the MP, one or more X-lines develop. The prevailing MSH flow ($v_L \sim -150$ km/s during the whole event) moves the X-lines and the magnetic flux ropes between them southward and dawnward. As the FTE closer to the nose of the magnetosphere moves away, a new X-line forms in its wake, which in turn creates a new flux rope. The v_L reversal from a larger negative value (~ -480 km/s) to a smaller positive value (~240 km/s) manifests the key signature of the presence of the south-dawnward moving X-line [*Moore et al.*, 2002; *Pu et al.*, 2005] ahead of the FTE. Furthermore, the −/+ bipolar polarity of FTE itself is consistent with an FTE moving south-dawnward as well. Assuming that in the frame of reference moving with the X-line, two reconnection jets were antisymmetric, it is easy to obtain that the X-line system moved as a whole roughly at $V_L \sim -120$ km/s. To estimate the motion of the FTE, we have tried to calculate its $\mathbf{V_{HT}}$. However, it could not be determined, likely because the FTE was still growing and very active, and there was no such a frame of reference in which the convection electric field vanished [*Sonnerup et al.*, 1987].

[8] The most important finding in this in situ measurement is that magnetic flux from all four possible magnetic topologies is present in the central region of the observed FTE. This cannot be reconciled with simple 2D models of reconnection, which only allow for open flux with one end connected to the northern or southern magnetosphere. We thus interpret the coexistence of four different magnetic topologies as the distinguishing feature of intrinsically 3D multiple X-line reconnection [*Fu et al.*, 1990; *Raeder*, 2006; *Tan et al.*, 2011].

[9] In Figure 3, we illustrate, by modifying and extending the picture of *Fu et al.* [1990], how four types of field line topologies are created in the MSXR process. In this figure, X-line 1 and 2 represent the southern/dawnward and the equatorial X-line, respectively. Red and blue lines indicate the MSP and MSH field lines, respectively. An FTE, and

the associated four types of field lines (in purple), are formed when X-line 1 moves away south-dawnward and reconnection takes place at X-line 2. The figure depicts how: (i) an open field line connected to the southern magnetosphere is produced by reconnection of an open field line from the first X-line reconnection with an MSP field line and an MSH field line; (ii) an open field line connecting to the northern hemisphere is created when two open field lines from the first X-line reconnection reconnect; (iii) a closed field line connecting both hemispheres is produced when an open field line from the first X-line reconnects with an MSP field line, and (iv) an MSH field line is created by reconnection of an open field line from the first X-line with a MSH field line.

[10] Figure 3 indicates that as the FTE moves across the MP, reconnection continues at the leading and trailing edges of the FTEs and profoundly alters the magnetic topology. In particular, field lines reconnect multiple times to increase the winding number of the flux that makes up the FTE. This process is a unique feature for 3D MSXR, which distinguishes it from all other proposed FTE mechanisms [*Scholer*, 1995]. On completion of the process, the FTE flux ropes contain a significant amount of closed flux in addition to open flux in the core region [*Oieroset et al*., 2011]. This is an important property, because the closed flux in the FTEs plays an important role in forming the low-latitude boundary layer with closed field lines [*Lee et al*., 1993], whereas it may contribute less to magnetospheric and ionospheric convection as the reconnection rate would indicate. Although the presence of multiple simultaneous reconnection sites may compensate for this, the local reconnection rate may not correspond to the cross polar cap potential, as is usually assumed in simple Faraday loop models. On the other hand, transport of mass and momentum into the magnetosphere may be larger than previously thought because ultimately more IMF flux is reconnected. Quantifying the balance of these processes calls for more multipoint observations and more realistic simulations.

[11] In summary, Double Star/TC-1 measurements of an in vivo FTE on 2004-04-07 present the first in situ evidence for coexistence of four types of magnetic topologies within the FTE flux rope. This knowledge of magnetic topologies of FTE flux ropes helps to improve our understanding of solar wind-magnetosphere coupling at the MP.

[12] **Acknowledgments.** This work was supported by the Chinese NSFC programs 41274167, 40731056, 40974095, and 10975012, the Chinese National Key Basic Research Science Foundation (2011CB811400), the National Science Foundation (ATM-0639658 and OCI-0749125), and NASA (NNX10AL07G). We thank C. Carr and H. Reme for providing the Double Star FGM and HIA data.

[13] First and second authors contributed equally.

References

Bogdanova, Y. V., et al. (2008), Formation of the low-latitude boundary layer and cusp under the northward IMF: Simultaneous observations by Cluster and Double Star, *J. Geophys. Res.*, *113*, A07S07, doi:10.1029/2007JA012762.

Carr, C., et al. (2005), The Double Star magnetic field investigation: Instrument design, performance and highlights of the first year's observations, *Ann. Geophys.*, *23*, 2713–2732.

Cooling, B. M. A., C. J. Owen, and S. J. Schwartz (2001), Role of the magnetosheath flow in determining the motion of open flux tubes, *J. Geophys. Res.*, *106*(A9), 18,763–18,775, doi:10.1029/2000JA000455.

Dorelli, J. C., and A. Bhattacharjee (2009), On the generation and topology of flux transfer events, *J. Geophys. Res.*, *114*, A06213, doi:10.1029/2008JA013410.

Eastwood, J. P., et al. (2012), Survival of flux transfer event (FTE) flux ropes far along the tail magnetopause, *J. Geophys. Res.*, *117*, A08222, doi:10.1029/2012JA017722.

Farrugia, C. J., et al. (1987a), Field and flow perturbations outside the reconnected field line region in flux transfer events: Theory, *Planet. Space Sci.*, *35*, 227–240.

Farrugia, C. J., et al. (1987b), Two-regime flux transfer events, *Planet. Space Sci.*, *35*, 737–744.

Fazakerley, A. N., et al. (2005), The Double Star plasma electron and current experiment, *Ann. Geophys.*, *23*, 2733–2756.

Fedder, J. A., et al. (2002), Flux transfer events in global numerical simulations of the magnetosphere, *J. Geophys. Res.*, *107*(A5), 1048, doi:10.1029/2001JA000025.

Fu, Z. F., L. C. Lee, and Y. Shi (1990), *A three-dimensional MHD simulation of the multiple X line reconnection process*, in *Physics of Magnetic Flux Ropes, Geophys. Monogr. Ser.*, vol. 58, edited by C. T. Russell, E. R. Priest, and L. C. Lee, pp. 515–519, AGU, Washington, D. C.

Hasegawa, H., et al. (2010), Evidence for a flux transfer event generated by multiple X-line reconnection at the magnetopause, *Geophys. Res. Lett.*, *37*, L16101, doi:10.1029/ 2010GL044219.

Khrabrov, A. V., and B. U. Ö. Sonnerup (1998), DeHofmann-Teller analysis, analysis methods for multi-spacecraft data, edited by G. Paschmann and P. W. Daly, ISSI Science Report, SR-001, 221-248.

Le, G., C. T. Russell, and H. Kuo (1993), Flux transfer events: spontaneous or driven?, *Geophys. Res. Lett.*, *20*, 791–794.

Lee, L. C., and Z. F. Fu (1985), A theory of magnetic flux transfer at the Earth's magnetopause, *Geophys. Res. Lett.*, *12*, 105–108.

Lee, L. C., et al. (1993), Topology of magnetic flux ropes and formation of fossil flux transfer events and boundary layer plasmas, *J. Geophys. Res.*, *98*(A3), 3943–3951, doi:10.1029/92JA02203.

Liu, Z. X., and Y. D. Hu (1988), Local reconnection caused by vortices in flow field, *Geophys. Res. Lett.*, *15*, 752–755.

Liu, Z. X., et al. (2005), The Double Star Mission, *Ann. Geophys.*, *23*, 2707–2712.

Moore, T. E., M.-C. Fok, and M. O. Chandler (2002), The dayside reconnection X line, *J. Geophys. Res.*, *107*(A10), 1332, doi:10.1029/2002JA009381.

Oieroset, M., et al. (2011), Direct Evidence for a Three-Dimensional Magnetic Flux Rope Flanked by Two Active Magnetic Reconnection X Lines at Earth's Magnetopause, *Phys. Rev. Lett.*, *107*(16), 16,5007.

Paschmann, G., et al. (1982), Plasma and magnetic field characteristics of magnetic flux transfer events, *J. Geophys. Res.*, *87*(A4), 2159–2168.

Phan, T. D., et al. (2004), Cluster observations of continuous reconnection at the magnetopause under steady interplanetary magnetic field conditions, *Ann. Geophys.*, *22*, 2355–2367.

Pu, Z. Y., et al. (2005), Double Star TC-1 observations of component reconnection at the dayside magnetopause: A preliminary study, *Ann. Geophys.*, *23*, 2889–2895.

Raeder, J. (2006), Flux transfer events: 1. Generation mechanism for strong southward IMF, *Ann. Geophys.*, *24*(1), 381–392.

Rastätter, L., et al. (2012), Scientific visualization to study flux transfer events at the Community Coordinated Modeling Center, *Adv. Space Res.*, *49*, 1623–1632.

Reme, H., et al. (2005), The HIA instrument on board the Tan Ce 1 Double Star near-equatorial spacecraft and its first results, *Ann. Geophys.*, *23*, 2757–2774.

Russell, C. T., and R. C. Elphic (1978), Initial ISEE magnetometer results: Magnetopause observations, *Space Sci. Rev.*, *22*, 681–715.

Scholer, M. (1988), Magnetic flux transfer at the magnetopause based on single X line bursty reconnection, *Geophys. Res. Lett.*, *15*(4), 291–294.

Scholer, M. (1995), Models of flux transfer events, in *Physics of the Magnetopause, Geophys. Monogr. Ser.*, vol. 90, edited by P. Song, B. U. Ö. Sonnerup, and M. Thomsen, pp. 235–245, AGU, Washington, D. C.

Sonnerup, B. U. Ö., and M. Scheible (1998), Minimum and maximum variance analysis, in *Analysis Methods for Multi-Spacecraft Data*, edited by G. Paschmann, and P. W. Daly, ISSI scientific Report SR-001, pp. 185–220, Int. Space Sci. Inst., Bern, Switzerland.

Sonnerup, B. U. Ö., et al. (1987), Magnetopause properties from AMPTE/IRM observations of the convection electric field: Method development, *J. Geophys. Res.*, *92*(A11), 12,137–12,159.

Sonnerup, B. U. Ö., G. Paschmann, and T.-D. Phan (1995), Fluid aspects of reconnection at the magnetopause, in *Physics of the Magnetopause*, edited by P. Song, B. U. Ö. Sonnerup, and M. F. Thomsen, AGU Geophys. Monogr. *90*, 167C180, AGU, Washington, D. C.

Tan, B., et al. (2011), Global-scale hybrid simulation of dayside magnetic reconnection under southward IMF: Structure and evolution of reconnection, *J. Geophys. Res.*, *116*, A02206, doi:10.1029/2010JA015580.

Trenchi, L., et al. (2011), TC-1 observations of a flux rope: Generation by multiple X line reconnection, *J. Geophys. Res.*, *116*, A05202, doi:10.1029/2010JA015986.

Zhang, H., et al. (2012), Generation and properties of in vivo flux transfer events, *J. Geophys. Res.*, *117*, A05224, doi:10.1029/ 2011JA017166.